

Provided for non-commercial research and education use.
Not for reproduction, distribution or commercial use.



This article appeared in a journal published by Elsevier. The attached copy is furnished to the author for internal non-commercial research and education use, including for instruction at the authors institution and sharing with colleagues.

Other uses, including reproduction and distribution, or selling or licensing copies, or posting to personal, institutional or third party websites are prohibited.

In most cases authors are permitted to post their version of the article (e.g. in Word or Tex form) to their personal website or institutional repository. Authors requiring further information regarding Elsevier's archiving and manuscript policies are encouraged to visit:

<http://www.elsevier.com/copyright>



Contents lists available at ScienceDirect

Journal of Industrial and Engineering Chemistry

journal homepage: www.elsevier.com/locate/jiec

Comparative study on nano-crystalline titanium dioxide catalyzed photocatalytic degradation of aromatic carboxylic acids in aqueous medium

V.G. Gandhi^a, M.K. Mishra^a, M.S. Rao^a, A. Kumar^c, P.A. Joshi^{a,*}, D.O. Shah^{a,b}^a Department of Chemical Engineering & Shah Schulman Center for Surface Science and Nanotechnology, Dharmsinh Desai University, College Road, Nadiad 387 001, Gujarat, India^b Center for Surface Science and Engineering, University of Florida, Gainesville, USA^c R&D Centre, Reliance Industries Limited, Baroda, Gujarat, India

ARTICLE INFO

Article history:

Received 1 July 2010

Accepted 2 September 2010

Available online 2 March 2011

Keywords:

Photocatalytic degradation
Nano-crystalline titanium dioxide
Aromatic carboxylic acids

ABSTRACT

The comparative study on titanium dioxide (TiO₂) catalyzed photocatalytic degradation (PCD) of aqueous aromatic carboxylic acids (phthalic acid, *o*-nitrobenzoic acid, *o*-chlorobenzoic acid and benzoic acid) was carried out in the presence of UV radiation using air. The TiO₂ catalyst, synthesized by sol-gel technique and calcined at 673 K, resulted ca. 100% anatase phase with 23 nm crystallite size and surface area of 37 m²/g. This catalyst was found to be efficient for PCD of phthalic acid, *o*-nitrobenzoic acid, *o*-chlorobenzoic acid and benzoic acid in aqueous medium. However, the reactivity and degradation pathway of these carboxylic acids were observed to be greatly influenced by the substituent group present in the aromatic ring. The order of degradation of aromatic carboxylic acids was found to be phthalic acid > *o*-nitrobenzoic acid > *o*-chlorobenzoic acid > benzoic acid. The aromatic carboxylic acids having electron withdrawing groups such as -COOH, -NO₂ and -Cl were comparatively more reactive for PCD than unsubstituted aromatic acid i.e., benzoic acid. The degradation of ortho substituted benzoic acids (having electron withdrawing groups) follows different mechanistic pathway than that of benzoic acid. Study of various operational parameters like effect of catalyst loading, initial concentration of phthalic acid and kinetics of phthalic acid PCD was also carried out in batch type photocatalytic reactor.

© 2011 The Korean Society of Industrial and Engineering Chemistry. Published by Elsevier B.V. All rights reserved.

1. Introduction

The aromatic carboxylic acids such as phthalic acid, *o*-nitrobenzoic acid, *o*-chlorobenzoic acid and benzoic acid are widely used as reactants or produced as main products or by-products in various chemical products like paints, pharma, dyes and fine chemicals. Benzoic acid and its chloro-, nitro-derivatives are mostly found in the waste water of pharma industries. Phthalic acid is found in the waste water of dyes and paint industries, where it is used in acylation, esterification, etc. The effluents generated by these industries contain significant amount of aromatic carboxylic acids. The aromatic carboxylic acids are highly stable and non-biodegradable pollutants, which need to be removed from waste water before disposal to natural water bodies due to the environmental restrictions and their hazardous effects on flora and fauna.

Considerable efforts have been made by many researchers to find appropriate technique for the removal of pollutants from

waste water. The most commonly used methods are adsorption techniques using activated carbon based adsorbents, organocatalysis, etc. [1–5], electrochemical method [6], microbiological decomposition [7] and chemical coagulation [8]. The adsorption process is cost effective method for waste water treatment, but the process only concentrate the contaminant from water onto a solid substrate causing secondary pollution problem [9]. Coagulation using alums, ferric salts, or limes is also a low cost process but disposal of sludge is an issue. Microbiological process suffers from slower rate of reaction.

In recent years, the TiO₂ catalyzed photocatalytic degradation (PCD) in the presence of UV radiation and air has attracted attention of researchers for remediation of hazardous pollutants in water. One of the advantages of PCD over conventional treatment techniques is degradation of a broad range of organic pollutants under mild operating conditions and complete mineralization [10]. The TiO₂ catalyzed PCD of various groups of organic pollutants like alcohols, phenols, carbonyls and carboxylic compounds, aromatics and halocarbons has been reported elsewhere [10–15].

The removal of several aliphatic carboxylic acids [16–18] as well as aromatic acids such as benzoic acid, polycarboxylic acids, salicylic acid, chlorobenzoic acids and many others [19–24] from

* Corresponding author. Tel.: +91 268 2520502; fax: +91 268 2520501.

E-mail address: pajoshi24@gmail.com (P.A. Joshi).

water using TiO₂ catalyzed PCD has been reported. Besides this, photocatalytic degradation of the higher aliphatic carboxylic acids such as branched C4 and C5 aliphatic acids using TiO₂ has also been studied [25]. A number of reports have been published on the effect of substituents and the molecular structure of organics on the degradation rate for TiO₂ catalyzed PCD [20,22,24,26,27]. However, the effect of substituents on the reactivity and degradation pathways of the aromatic carboxylic acids for TiO₂ catalyzed PCD has not been studied in detail. The present work focuses on a comparative study of TiO₂ catalyzed PCD of unsubstituted aromatic carboxylic acid i.e., benzoic acid and its ortho substituted (–COOH, –NO₂ and –Cl) derivatives studying the influence of molecule structure on the kinetics and mechanistic pathway. A detail study on the effect of catalyst characteristics, important reaction parameters, PCD kinetics of phthalic acid was carried out.

2. Experimental

2.1. Chemicals

Titanium tetra *iso*-propoxide (98%) was purchased from Spectrochem Pvt. Ltd., Mumbai, India and aqueous ammonia (25%), benzoic acid (99%), phthalic acid (99%), *o*-chlorobenzoic acid (99%), *o*-nitrobenzoic acid (99%) were obtained from s.d. fine chem. Ltd., Mumbai, India. Methanol (99%) was obtained from Merck Ltd., Mumbai, India.

2.2. Synthesis and characterization of TiO₂ catalyst

The TiO₂ catalyst was synthesized by sol–gel technique [28] using titanium tetra *iso*-propoxide (TTIP) as precursor. Aqueous ammonia was added drop wise in TTIP–methanol solution (20 wt.% solution) under continuous stirring till the solution achieved pH of 9–10. The resulting gel was stirred for 2 h at room temperature. The gel was filtered, washed with methanol and dried at room temperature for 2 h and then at 353 K for 12 h. The dried gel was calcined for 4 h at different temperatures, 673 K (T-673), 723 K (T-723), 823 K (T-823) and 923 K (T-923).

The crystalline nature, type and composition of phases and the crystallite size of TiO₂ catalysts were measured by XRD analysis using X-ray diffractometer (Bruker D-8 Advance X-ray powder Diffractometer) having Cu K α radiation ($\lambda = 1.5418 \text{ \AA}$) with nickel filter and scintillation detector. The sample was scanned in 2θ range of 15–90° with a scanning rate of 0.02° s⁻¹. The anatase phase fraction was calculated using following equation [29]:

$$X_A (\%) = \frac{1}{[1 + 1.265(I_R/I_A)]} \times 100 \quad (1)$$

where I_A denotes the intensity of strongest anatase reflection ($2\theta = 25.5^\circ$) and I_R is the intensity of the strongest rutile reflection ($2\theta = 27.5^\circ$).

Crystallite size of each phase was determined from the peak of maximum intensity of the phase using Scherrer formula with a shape factor (K) of 0.9 [30] as given below

$$\text{Crystallite size} = \frac{K\lambda}{W} \cos \theta \quad (2)$$

where $W = W_b - W_s$; W_b is the broadened profile width of experimental sample and W_s is the standard profile width of reference silicon sample.

The FT-IR study of catalysts was carried out using FT-IR spectrophotometer (IRPrestige-21, Shimadzu) in DRS (diffuse reflectance system) by mixing the sample with dried KBr in 1:20 weight ratio in the range of 400–4000 cm⁻¹ with a resolution of 4 cm⁻¹.

The thermal analysis (TGA–DTG) of the uncalcined sample was carried out by Mettler Thermal Analyzer, TA4000, in the range of 323–1173 K with a heating rate of 283 K/min under nitrogen flow (100 cm³/min).

N₂ adsorption–desorption isotherm study of TiO₂ samples was carried out using NOVA 1000e surface area analyzer. The surface area was calculated by using BET equation [31].

2.3. Photocatalytic degradation of aromatic carboxylic acids using TiO₂

The photocatalytic degradation of phthalic acid, *o*-nitrobenzoic acid, *o*-chlorobenzoic acid and benzoic acid was carried out using synthesized TiO₂ catalyst in water in the presence of UV light and air. 250 ml aqueous solution of the carboxylic acid (100–300 mg/l) was taken in a photocatalytic reactor equipped with a magnetic stirrer and water cooling jacket, UV light source (Phillips High Pressure Mercury lamp, 120 W). The TiO₂ catalyst (1–5 g/l) was added in the reactor and reaction was carried out at constant temperature (303 K) under continuous stirring, aeration and irradiation of UV light. The reaction progress, i.e., degradation of the acid, was monitored by analyzing the samples collected at different time intervals using High Performance Liquid Chromatograph (Dionex Ultimate 3000) with C8 column (Acclaim 120, 5 μm , 120 \AA , 4.6 mm \times 250 mm).

The operating conditions for HPLC analysis are acetonitrile–water eluents (50:50 for the analysis of benzoic acid, phthalic acid and *o*-chloro benzoic acid, 70:30 for the analysis of *o*-nitro and benzoic acid), flow rate of 1 ml/min and 235 nm wave length of photodiode array detector at constant column temperature of 298 K. The reaction intermediates were identified by HPLC analysis. The adsorption of aromatic carboxylic acids on TiO₂ catalyst was measured by treating 0.25 g TiO₂ catalyst with 100 ml solutions of carboxylic acid (100 mg/l) in the absence of light for 1 h. The photolysis of the aromatic carboxylic acids (100 ppm solution) was also examined by illuminating the aqueous solution of compounds for 1 h in the absence of TiO₂ catalyst.

3. Results and discussion

3.1. Characterization of TiO₂ catalyst

Before calcination, the synthesized titanium hydroxide was amorphous and after calcination at 673 K, predominantly (ca. 100%) anatase phase was formed in the sample (T-673) showing characteristic peak of anatase at 2θ value of 25.5° (Fig. 1). There was slight change in phase composition (89% anatase and 11%

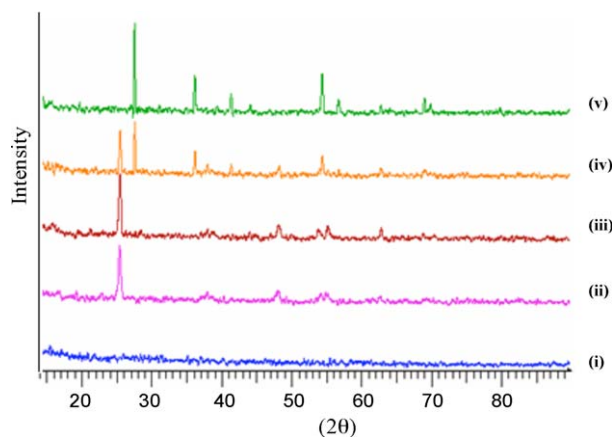


Fig. 1. XRD pattern of TiO₂ samples (i) before calcination, after calcination at (ii) 673 K, (iii) 723 K, (iv) 823 K and (v) 923 K.

Table 1

Crystal phase composition and crystallite size of TiO₂ samples calcined at 673, 723, 823 and 923 K.

Samples	% Phase		Crystallite size (nm)		BET surface area (m ² /g)
	Anatase	Rutile	Anatase	Rutile	
T-673	100	0	23	–	37
T-723	89	11	24	53	36
T-823	40	60	30	35	16
T-923	0	100	–	37	7

rutile) of the sample (T-723) calcined at 723 K; however, calcination at 823 K resulted into formation of 60% rutile (peak at 2θ value of 27.5°) and 40% anatase phase. Further increase in calcination temperature increases the amount of rutile phase giving ca. 100% rutile phase at 923 K. The anatase phase has been reported to be catalytically more active phase for photocatalysis [32], therefore, the catalysts T-673 and T-723 are supposed to be more active for PCD of aromatic carboxylic acids. The average crystallite size of anatase phase of TiO₂ (Table 1) increases and that of rutile phase decreases with increasing calcination temperature. The increase of crystallite size of anatase phase is attributed to the crystal growth at high temperature and sintering of the crystallites. The TiO₂ samples, calcined at lower temperature (673 K and 723 K), are nanocrystalline (23 and 24 nm) with predominantly anatase phase [33].

The FT-IR spectra (Fig. 2) of TiO₂ samples (T-673 and T-723) calcined at 673 and 723 K show a broad band in the range of 3000–3800 cm⁻¹ (ν_{OH}), which is attributed to the hydroxyl groups present in TiO₂ (titanol, >Ti–OH) and adsorbed water. The peak at 1630 cm⁻¹ is attributed to bending mode of –OH of titanol and water. It depicts that T-673 and T-723 catalysts are enriched with surface hydroxyl groups as compared to T-823 and T-923 samples.

The thermal analysis (TGA–DTG) of TiO₂ gives total weight loss of 15 wt.% (Fig. 3). The TGA–DTG graphs show three steps of weight loss. The first step (323–573 K) is attributed to loss of free adsorbed water and the water adsorbed on TiO₂ surface by hydrogen bonding and the solvents (methanol and *iso*-propanol, formed during hydrolysis of titanium tetra *iso*-propoxide). The second step (613–673 K) is due to crystallization to anatase phase and the third step (at ~873 K) for phase transformation of anatase to rutile phase. The TGA–DTG analysis clearly indicates the temperatures required for getting anatase phase of titanium dioxide is 673 K and therefore, the sample, after calcination at 673 K, contains predominantly 100% anatase phase.

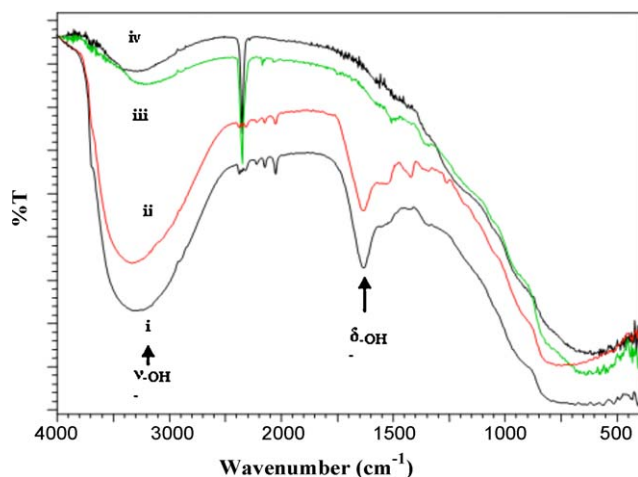


Fig. 2. FT-IR spectrum of TiO₂ samples calcined at (i) 673 K, (ii) 723 K, (iii) 823 K and (iv) 923 K.

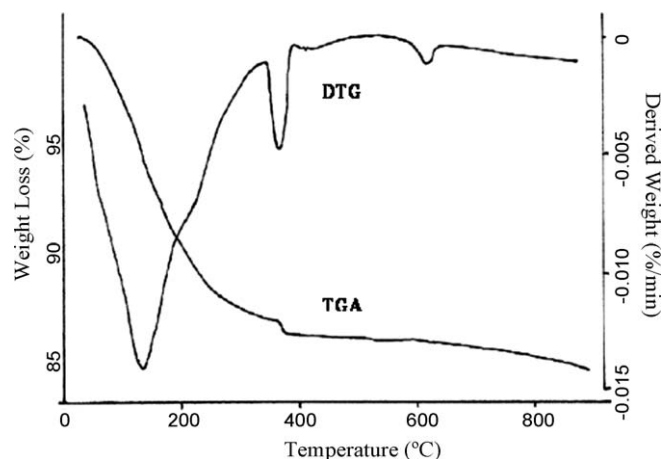


Fig. 3. TGA–DTG profile of Ti(OH)₄ sample.

Table 2

pK_a values of aromatic carboxylic acids, % adsorption of aromatic carboxylic acids over TiO₂ and rate constants of TiO₂ catalyzed PCD of aromatic carboxylic acids.

Aromatic carboxylic acids	pK_a value	% Adsorption after 1 h	Rate constant (h ⁻¹)
Phthalic acid	2.9	4.5	1.08
<i>o</i> -Nitrobenzoic acid	2.2	3.0	0.42
<i>o</i> -Chlorobenzoic acid	2.9	2.5	0.17
Benzoic acid	4.2	0.5	0.10

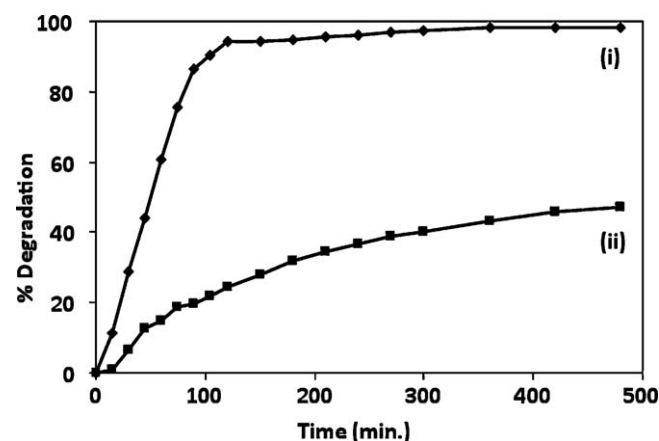


Fig. 4. Degradation of phthalic acid with TiO₂ (i) calcined at 673 K and (ii) 723 K (phthalic acid concentration = 100 mg/l, catalyst amount = 2.5 g/l).

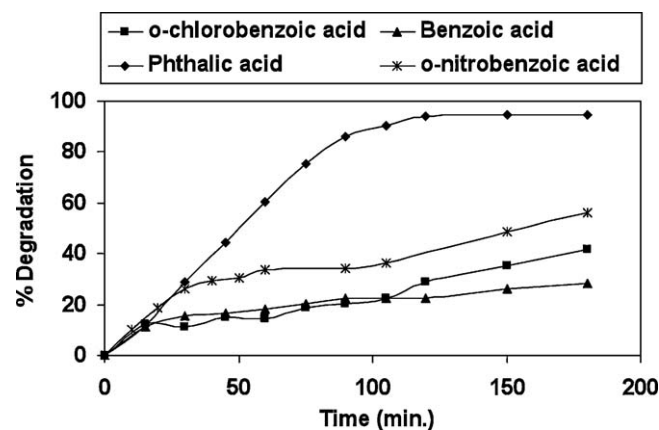


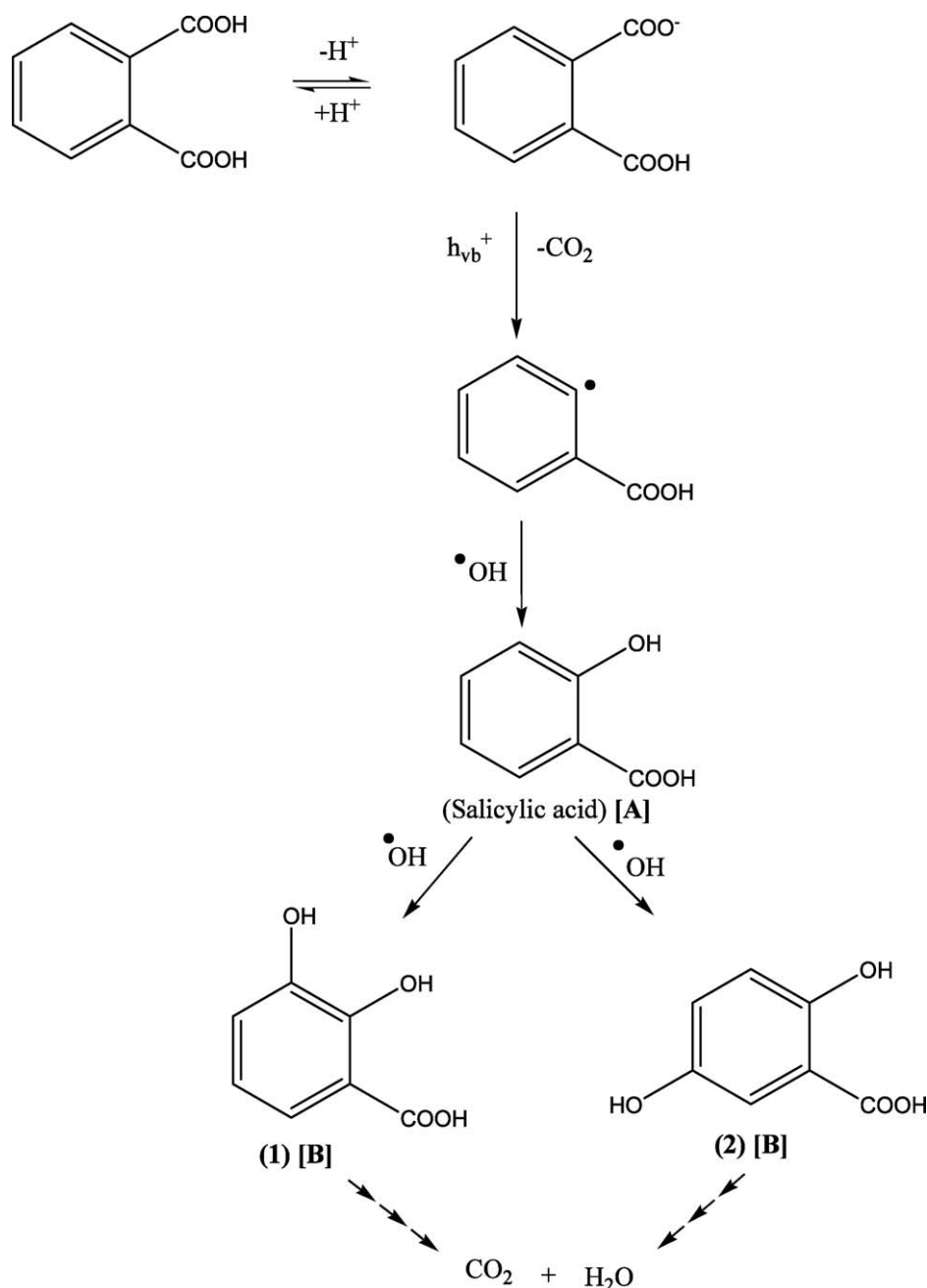
Fig. 5. Degradation of various aromatic carboxylic acids with time (acid concentration = 100 mg/l, catalyst amount = 2.5 g/l).

The BET surface area of the TiO₂ samples, T-673 and T-723, was 37 and 36 m²/g respectively, which decreased to 16 and 7 m²/g for the samples T-823 and T-923 respectively. The decrease in surface area with calcination temperature is attributed to increase in crystallite size due to sintering of crystallites and pores (Table 1).

3.2. PCD of aromatic carboxylic acids using nano-crystalline TiO₂

The direct photolysis of the aromatic carboxylic acids (phthalic acid, *o*-nitrobenzoic acid and *o*-chlorobenzoic acid), in the absence of TiO₂ catalyst, did not show any reduction in the concentration proving that the compounds are photostable. In the absence of UV light, the adsorption of these acids on TiO₂ was observed to be in the range of 0.5–4.5% (Table 2). The adsorption of the unsubstituted acid (benzoic acid) was lower (0.5%), whereas significant amount (2.5–

4.5%) of ortho substituted acids (phthalic acid, *o*-nitrobenzoic acid and *o*-chlorobenzoic acid) was adsorbed (Table 2). This variation is attributed to the ionization extent of the acids to respective carboxylates i.e., stability of carboxylates. The adsorption of carboxylic acids (R–COOH) over TiO₂ surface can be considered as electrostatic interaction of carboxylate ions (R–COO[−]) with titanol (>Ti–OH) or protonated titanol (>Ti–OH₂⁺). Benzoic acid gives lesser amount of benzoate ions in water (pK_a = 4.2) (Table 2), and therefore, results to very less adsorption of benzoic acid on TiO₂. The less adsorption of benzoic acid over TiO₂ has been reported in earlier studies on photocatalytic degradation of benzoic acid [21]. The ortho substituted aromatic carboxylic acids (phthalic acid, *o*-nitrobenzoic acid and *o*-chlorobenzoic acid) are comparatively more adsorbed as the extent of ionization of these acids is more (pK_a = 2.2–2.9) (Table 2) and they remain in ionized form or carboxylate ions. The effect of



Scheme 1. Mechanistic pathway of titanium dioxide catalyzed photodegradation of phthalic acid ([A] = confirmed by HPLC analysis, [B] = expected to be formed).

adsorption of these compounds on the degradation rate and the pathways were observed to be important, which will be discussed in the next section.

3.2.1. Effect of calcination temperature on PCD activity

The TiO₂ samples, T-673 and T-723, possess similar characteristics (evident from XRD, FT-IR, and surface area analysis), therefore, T-723 may have similar catalytic activity as T-673. The T-923 contains mainly rutile phase, which is catalytically less active. Therefore, to study the effect of calcination temperature and catalyst characteristics on photocatalytic activity, the T-673 and T-823 samples were tested for PCD of phthalic acid. The T-673 was found to be more active giving >90% phthalic acid degradation within 2 h, while T-823 showed very less activity (Fig. 4). The less activity of T-823 is attributed to decreased amount of anatase phase, crystallites, less hydroxyl groups and smaller surface area. The calcination at low temperature (673 K) produces highly active TiO₂ catalyst containing ca.100% anatase phase with smaller crystallite size and higher surface area. This catalyst is enriched with –OH groups, which helps in adsorption of phthalic acid. Furthermore, –OH groups play important role in photocatalysis facilitating electron transfer between surfaces and reacting molecules [12,20]. For further study on TiO₂ catalyzed PCD of aromatic carboxylic acids, T-673 catalyst was selected.

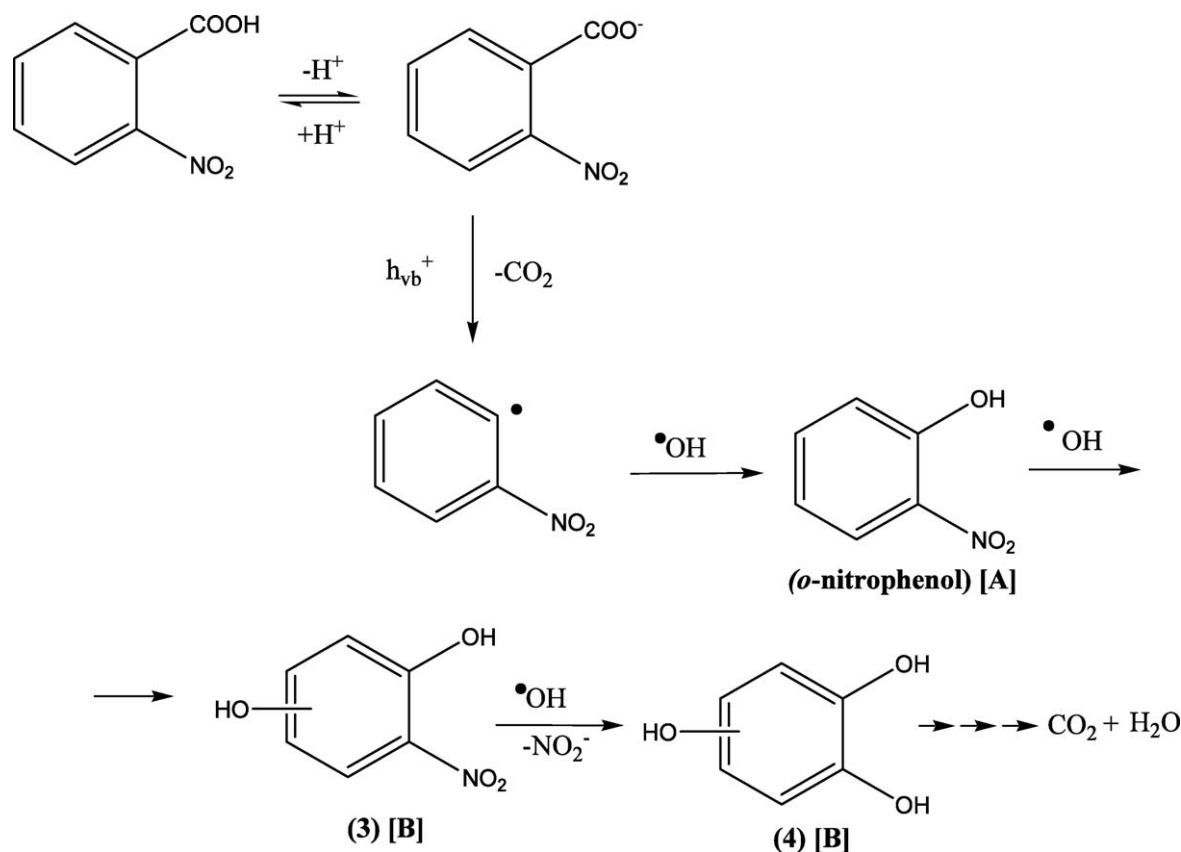
3.2.2. PCD of aromatic carboxylic acids and effect of substituents on their reactivity and mechanism of degradation

The T-673 was found to be active for PCD of phthalic acid, *o*-nitrobenzoic acid, *o*-chlorobenzoic acid and benzoic acid showing significant degradation in water (Fig. 5). However, PCD of phthalic acid was comparatively faster resulted >90% degradation within 3 h. The *o*-nitrobenzoic acid and *o*-chlorobenzoic acid degradation was slower with 42% and 38% degradation after 3 h, respectively.

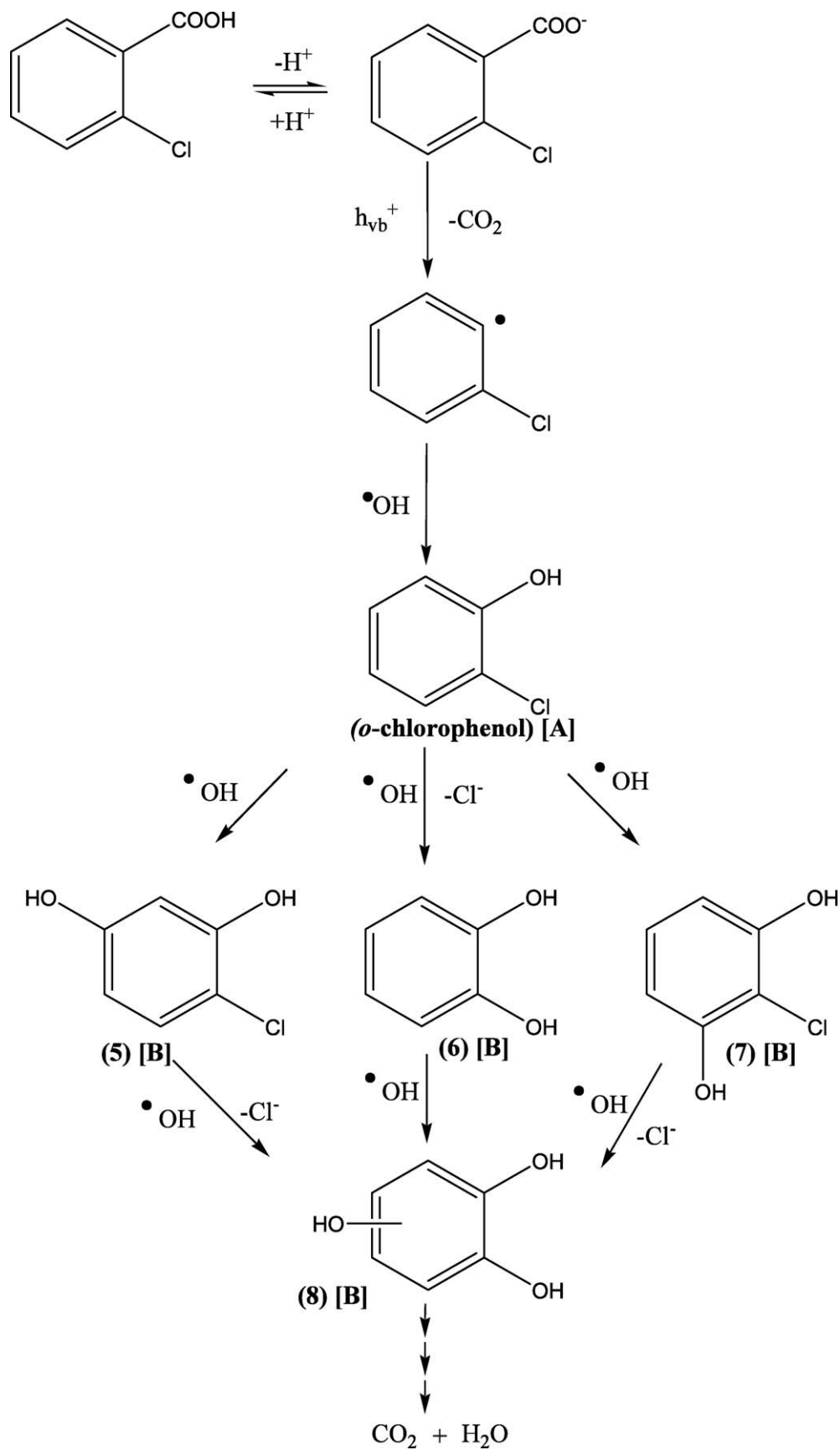
The rate of degradation of benzoic acid was slow with 28% degradation found after 3 h. The variation in degradation rates of these acids is ascribed to their reactivity, which is influenced by the nature of substituents present on the aromatic ring. The order of reactivity of the aromatic carboxylic acids for TiO₂ catalyzed photodegradation was found to be as follows:

Benzoic acid < *o*-chlorobenzoic acid < *o*-nitrobenzoic acid < phthalic acid.

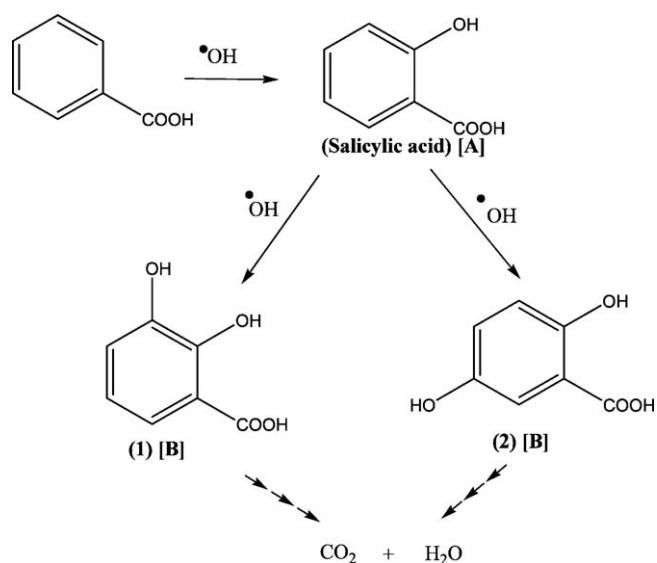
It was observed that the electron withdrawing substituents (groups having –I effect such as –COOH, –NO₂, –Cl) present at ortho position enhance the reactivity of the carboxylic acid for PCD. The unsubstituted acid (benzoic acid) was least reactive for TiO₂ catalyzed PCD. The fast degradation of phthalic acid (rate constant = 1.08 h⁻¹) is attributed to its more adsorption (4.5%) on TiO₂ surface (Table 2) as phthalate ions (electron donor). Surface adsorption of the electron donor to TiO₂ surface plays a significant role in determining the photoreactivity [12]. Besides this, the surface adsorption of phthalic acid is also facilitated by its surface complex formation with TiO₂ surface as the ortho-substituted benzene derivatives form chelating complex with surface >Ti–OH (titanol) of TiO₂. The chelating complex of phthalic acid with TiO₂ surface enhances the degradation rate accelerating the electron transfer from conduction band to acceptor in solution [34]. The *o*-chlorobenzoic acid and *o*-nitrobenzoic acid degradation rate was slower (0.42 and 0.17 h⁻¹ respectively) than phthalic acid as they differ in adsorption property showing lesser adsorption of 2.5 and 3.0% respectively (Table 2). It may be because of the presence of unsuitable groups (–NO₂ and –Cl) at ortho position to –COOH group, which do not help in forming chelating complex and to be strongly adsorbed on titanium dioxide as phthalic acid does. However, these groups stabilize the carboxylates (electron donors), which are adsorbed with TiO₂ surface by electrostatic interaction. The benzoic acid shows very slow degradation (rate



Scheme 2. Mechanistic pathway of titanium dioxide catalyzed photodegradation of *o*-nitrobenzoic acid ([A] = confirmed by HPLC analysis, [B] = expected to be formed).



Scheme 3. Mechanistic pathway of titanium dioxide catalyzed photodegradation of *o*-chlorobenzoic acid ([A] = confirmed by HPLC analysis, [B] = expected to be formed).



Scheme 4. Mechanistic pathway of titanium dioxide catalyzed photodegradation of benzoic acid ([A] = confirmed by HPLC analysis, [B] = expected to be formed).

constant = 0.1 h^{-1}) (Table 2) as benzoic acid was observed to be very less adsorbed on TiO_2 (0.5%) than ortho substituted acids. Furthermore, the single isolated carboxylate groups do not form strong surface complexation [35].

In PCD of phthalic acid, the salicylic acid was identified as major intermediate. The formation of salicylic acid indicates that phthalic acid first undergoes Kolbe's decarboxylation resulting into a free radical, which reacts with $\cdot\text{OH}$ radical (Scheme 1). Salicylic acid may react with $\cdot\text{OH}$ radicals to form 2,3-dihydroxy and 2,5-dihydroxy benzoic acids (1 and 2), which are reported to be reactive intermediate for ring opening reactions and finally oxidized to carbon dioxide and water [19]. The 2,3-dihydroxy benzoic acid and 2,5-dihydroxy benzoic acid were not observed by HPLC analysis, which may be because of their fast conversion to open chain compounds by ring opening of aromatic ring.

In PCD of *o*-nitrobenzoic acid and *o*-chlorobenzoic acid, *o*-nitro and *o*-chloro phenols formation was observed respectively, which indicates that these intermediate products were also formed by Kolbe's decarboxylation followed by reaction of $\cdot\text{OH}$ radicals (Scheme 2 and 3). The *o*-nitrophenol may undergo hydroxylation reactions to form di-hydroxy nitrobenzene (3) and finally tri-hydroxy benzene derivative (4) resulting to finally carbon dioxide and water. The TiO_2 catalyzed PCD of indigo and indigo carmine was reported to be giving *o*-nitrobenzoic acid as intermediate, which follows similar pathway of degradation [36]. The *o*-chlorophenol may also undergo hydroxylation reactions to form 2,4-dihydroxy chlorobenzene (5) and 2,6-dihydroxy chlorobenzene (7) [23]. Furthermore, the *o*-chlorophenol may also form catechol (6) by replacement of Cl group with $\cdot\text{OH}$ radical. These intermediates are degraded finally to carbon dioxide and water.

The PCD mechanism of benzoic acid (Scheme 4) was found to be different from that of ortho substituted benzoic acids (phthalic acid, *o*-nitrobenzoic acid and *o*-chlorobenzoic acid). The benzoic acid being less adsorbed over titanium dioxide undergoes reaction with $\cdot\text{OH}$ radicals in the solution followed by decarboxylation. The benzoic acid reacts with $\cdot\text{OH}$ radical to form salicylic acid as intermediate, which undergoes photodegradation as discussed earlier.

It was observed that the ortho substituted aromatic carboxylic acids (surface adsorbed electron donors) were degraded by photo Kolbe's decarboxylation followed by reactions of $\cdot\text{OH}$ radicals, whereas benzoic acid (less adsorbed) undergoes substitution reaction with $\cdot\text{OH}$ radicals followed by decarboxylation. The

degradation of ortho substituted acids by initial step of direct hydroxylation (substitution reaction with $\cdot\text{OH}$ radicals) may also be obstructed as the aromatic nucleus is highly deactivated (two electron withdrawing groups are present). The benzoic acid is comparatively more reactive for this reaction as only one electron withdrawing $-\text{COOH}$ group is present.

In order to examine the complete degradation of the compounds and their intermediates, the reactions were monitored till 8 h by HPLC. The phthalic acid was almost completely degraded and no peaks for salicylic acid or any other intermediates were observed after 4 h showing complete degradation. In case of benzoic acid and *o*-nitro and *o*-chloro benzoic acids, complete degradation of compounds and intermediates was found after 6 h.

3.3. Effect of initial concentration of phthalic acid and kinetic study

The PCD of phthalic acid was found to be dependent on the initial concentration (Fig. 6). At lower initial concentration (50 mg/l), the degradation amount was very less, which is due to less availability of reacting molecules around the surface sites. The highest amount of degradation was occurred at initial concentration of 100 mg/l and further increase in concentration does not change the degradation amount as the surface sites gets saturated with increased amount of molecules. However, with increasing initial concentration of phthalic acid (from 100 to 300 mg/l), the degradation rate was found to be decreasing (Fig. 7). The effect of the initial concentration on phthalic acid PCD rate was described by pseudo-first order kinetics. This is simplified in terms of Langmuir–Hinshelwood model modified to accommodate reactions occurring at solid liquid interface and the final form of the

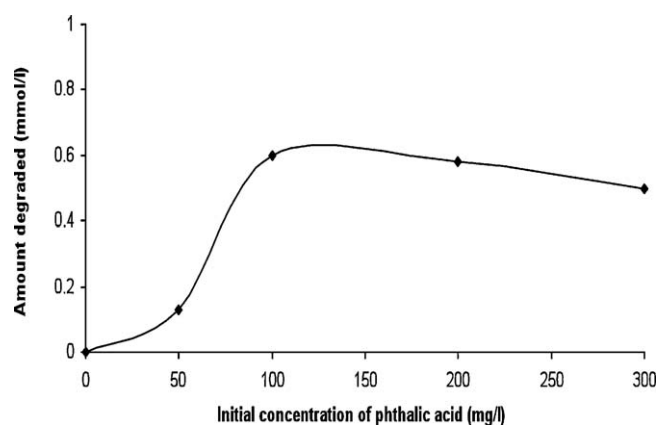


Fig. 6. Effect of initial concentration of phthalic acid on the degradation amount (catalyst amount = 2.5 g/l, reaction time = 3 h).

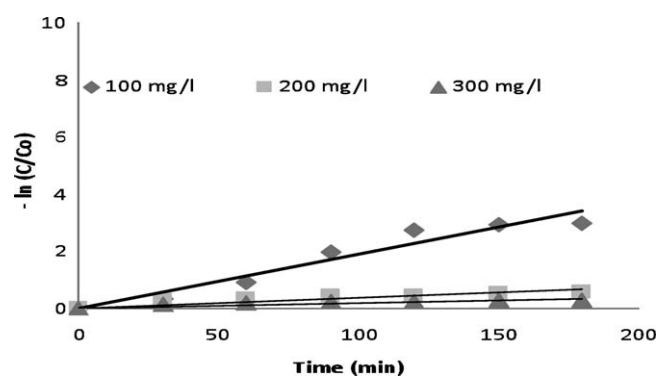


Fig. 7. Kinetics of phthalic acid PCD at different initial concentrations (catalyst amount = 2.5 g/l, reaction time = 3 h).

Table 3

Reaction rate constants of PCD of aromatic carboxylic acids at different initial concentrations of phthalic acid.

Concentration of phthalic acid (mg/l)	k' (h^{-1})
100	1.08
200	0.18
300	0.12

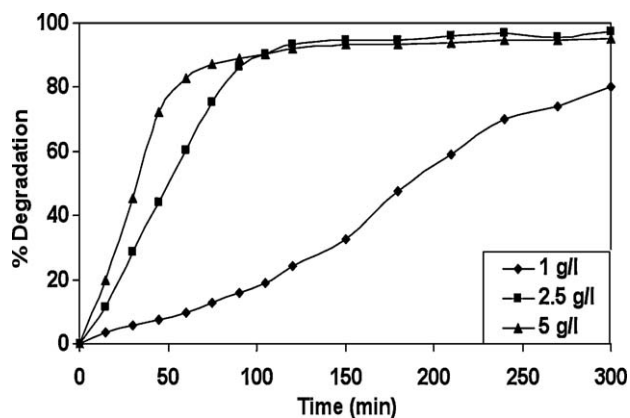


Fig. 8. Effect of catalyst loading on PCD of phthalic acid (phthalic acid concentration = 100 mg/l, reaction time = 6 h).

expression can be represented as [37–39]:

$$-\ln(C/C_0) = k_r K t = k' t \quad (3)$$

where C_0 is the initial concentration of phthalic acid at time $t = 0$ and C is the concentration of phthalic acid at reaction time t . The semi-logarithmic plot of $[-\ln(C/C_0)]$ versus time gives straight line indicating that the photocatalytic degradation of phthalic acid in aqueous titanium dioxide followed a first order kinetic (Fig. 7). The slope of the straight line gives the value of reaction rate constant, k' (h^{-1}). K is the equilibrium constant for adsorption of the pollutant on titanium dioxide particles and k_r is the limiting rate of the reaction after maximum coverage under the experimental conditions. The rate constant decreases from 1.08 to 0.12 h^{-1} with increase in the initial concentration of phthalic acid from 100 to 300 mg/l (Table 3). This may be due to higher concentration of phthalic acid molecules in the solution around the surface sites. At the surface of TiO_2 , the reaction occurs between the surface active sites and adsorbed phthalic acid molecules. When the initial concentration of phthalic acid is high, the numbers of available active sites would be less because of more competitive adsorption of phthalic acid on TiO_2 . The intensity of light, illumination period and the amount of generated oxygen active species ($\text{O}_2^{\bullet-2}$ and $\bullet\text{OH}$ radicals) are constant. So, at higher initial concentration, the amount of active sites and active species ($\bullet\text{OH}$ and $\text{O}_2^{\bullet-2}$) are less, which lowers the degradation rate. Similar effect has also been explained by Wei and Wan [40] and Gautam et al. [41] in photocatalytic degradation of phenol and 4-nitroaniline respectively.

3.4. Effect of catalyst dose

The extent of degradation of phthalic acid increases on increasing the catalyst amount (Fig. 8) and maximum degradation (98%, after 8 h) of phthalic acid was obtained at catalyst dose of 2.5 g/l. The higher dosing of catalyst slightly decreased the degradation rate of phthalic acid. This may be because of increase in opacity of the solution, which reduces the transmission intensity

of the radiation in bulk of solution and over a period of time, very less availability of pollutants around the catalytic sites for degradation.

4. Conclusions

The nano-crystalline titanium dioxide catalyst, synthesized by sol-gel technique and after calcination at 673 K, was found to be efficient for photodegradation of various aromatic carboxylic acids (benzoic acid, phthalic acid, *o*-chlorobenzoic acid and *o*-nitrobenzoic acid) in the presence of UV light. The microstructures of TiO_2 and reaction parameters affect the photocatalytic degradation of phthalic acid. The TiO_2 having smaller crystallite size of anatase phase ($\sim 100\%$), enriched with surface $-\text{OH}$ groups and higher surface area was more active for PCD. The reactivity of the aromatic carboxylic acids toward TiO_2 catalyzed PCD is affected by the nature of substituents present on the aromatic ring. The aromatic carboxylic acids having electron withdrawing groups ($-\text{COOH}$, $-\text{NO}_2$, $-\text{Cl}$, etc.) present at ortho position of aromatic ring, are highly reactive for PCD. The order of degradation of aromatic carboxylic acids was found to be phthalic acid > *o*-nitrobenzoic acid > *o*-chlorobenzoic acid > benzoic acid. Among the studied aromatic acids, phthalic acid was observed to be more reactive for TiO_2 catalyzed PCD, which is attributed to its higher sorption on TiO_2 .

Acknowledgements

The authors are thankful to Vice-chancellor, Dharmsinh Desai University, to provide valuable supports. We also wish to thank R&D Centre, Reliance Industries, Baroda Limited for providing analytical support.

References

- [1] V.K. Gupta, P.J.M. Carrott, M.M.L. Ribeiro Carrott, Suhas, Crit. Rev. Environ. Sci. Technol. 39 (2009) 783.
- [2] H.A. Patel, H.C. Bajaj, R.V. Jasra, Ind. Eng. Chem. Res. 48 (2009) 1051.
- [3] M. Arami, N.Y. Limaee, N.M. Mahmoodi, N.S. Tabrizi, J. Colloid Interface Sci. 288 (2005) 371.
- [4] M. Arami, N.Y. Limaee, N.M. Mahmoodi, N.S. Tabrizi, J. Hazard. Mater. B 135 (2006) 171.
- [5] M. Arami, N.Y. Limaee, N.M. Mahmoodi, Chemosphere 65 (2006) 1999.
- [6] A.G. Vlyssides, M. Loizidou, P.K. Karlis, A.A. Zorpas, D. Papaioannou, J. Hazard. Mater. 70 (1999) 41.
- [7] C.L. Pearce, J.R. Lloyd, J.T. Guthrie, Dyes Pigm. 58 (2003) 179.
- [8] S. Venkata Mohan, P. Sailaja, M. Srimurali, J. Karthikeyan, Environ. Eng. Policy 1 (1999) 149.
- [9] Z. Aksu, Process Biochem. 40 (2005) 997.
- [10] A. Mills, R.H. Davies, D. Worsley, Chem. Soc. Rev. 22 (1993) 417.
- [11] D.F. Ollis, E. Pellizzetti, N. Serpone, Environ. Sci. Technol. 25 (1991) 1523.
- [12] M.R. Hoffmann, S.T. Martin, W. Choi, D.W. Bahnemann, Chem. Rev. 95 (1995) 69.
- [13] D.S. Bhatkhande, V.G. Pangarkar, A.A.C.M. Beenackers, J. Chem. Technol. Biotechnol. 77 (2001) 102.
- [14] O. Legrini, E. Oliveros, A.M. Braun, Chem. Rev. 93 (1993) 671.
- [15] S.H. Song, M. Kang, J. Ind. Eng. Chem. 14 (2008) 785.
- [16] J.-M. Herrmann, H. Tahiri, C. Guillard, P. Pichat, Catal. Today 54 (1999) 131.
- [17] C. Guillard, J. Photochem. Photobiol. A: Chem. 135 (2000) 65.
- [18] A.D. Modestov, O. Lev, J. Photochem. Photobiol. A: Chem. 12 (1998) 261.
- [19] A.A. Ajmera, S.B. Sawant, V.G. Pangarkar, A.A.C.M. Beenackers, Chem. Eng. Technol. 25 (2002) 173.
- [20] K. Chhor, J.F. Bocquet, C. Colbeau-Justin, Mater. Chem. Phys. 86 (2004) 123.
- [21] T. Velegraki, D. Mantzavinos, Chem. Eng. J. 140 (2008) 15.
- [22] D. Vione, C. Minero, V. Maurino, M.E. Carloti, T. Picatotto, E. Pelizzetti, Appl. Catal. B: Environ. 58 (2005) 79.
- [23] H. Tahiri, Y.A. Ichou, J.-M. Herrmann, J. Photochem. Photobiol. A: Chem. 114 (1998) 219.
- [24] A. Assabane, Y.A. Ichou, H. Tahiri, C. Guillard, J.-M. Herrmann, Appl. Catal. B: Environ. 24 (2000) 71.
- [25] N. Serpone, J. Martin, S. Horikoshi, H. Hidaka, J. Photochem. Photobiol. A: Chem. 169 (2005) 235.
- [26] K. Tanaka, W. Luesaiwong, T. Hisanaga, J. Mol. Catal. A: Chem. 122 (1997) 67.
- [27] A.M. Peiró, J.A. Ayllón, J. Peral, X. Doménech, Appl. Catal. B: Environ. 30 (2001) 359.
- [28] M.K. Mishra, B. Tyagi, R.V. Jasra, Ind. Eng. Chem. Res. 42 (2003) 5727.
- [29] S. Rengaraj, X.Z. Li, J. Mol. Catal. A: Chem. 243 (2006) 60.

- [30] B.D. Cullity, S.R. Stock, Elements of X-ray Diffraction, Prentice Hall, Upper Saddle River, NJ, 2001.
- [31] S.J. Gregg, K.S.W. Sing, Adsorption, Surface Area and Porosity, 2nd ed., Academic Press, New York, 1982.
- [32] S. Cu, B.Y. Hong, C.M. Tseng, Catal. Today 96 (2004) 119.
- [33] S. Kumar, R. Chandra, Opt. Mater. 27 (2005) 1346.
- [34] J. Moser, S. PUNCHIHewa, P.P. Infelta, M. Gratzel, Langmuir 7 (1991) 3012.
- [35] S. Tunesi, M.A. Anderson, Langmuir 8 (1992) 487.
- [36] M. Vautier, C. Guillard, J.-M. Herrmann, J. Catal. 201 (2001) 46.
- [37] C.S. Turchi, D.F. Ollis, J. Catal. 122 (1990) 178.
- [38] H. Al-Ekabi, N. Serpone, J. Phys. Chem. 92 (1988) 5726.
- [39] B.B. Swarnalatha, Y. Anjaneyulu, J. Mol. Catal. A: Chem. 223 (2004) 161.
- [40] Y.T. Wei, C. Wan, J. Photochem. Photobiol. A: Chem. 69 (1992) 241.
- [41] S. Gautam, S.P. Kamble, S.B. Sawant, V.G. Pangarkar, Chem. Eng. J. 110 (2005) 129.